KSME

Springer

Journal of Mechanical Science and Technology 35 (5) 2021

Original Article
DOI 10.1007/s12206-021-0410-x

Keywords:
· Urban railway vehicle
· Brake disc
· Brake pad
· Squeal noise
· Complex eigenvalue analysis

Correspondence to:
Sungjin Choi
sjchoi@katech.re.kr

Citation:
Ahn, S., Nam, C., Choi, S., An, D., Kim, I., Seo, K., Sohn, C. (2021). A study on squeal noise reduction considering the pad shape of the disc brake system for urban railway vehicles. Journal of Mechanical Science and Technology 35 (5) (2021) 1923~1933.
http://doi.org/10.1007/s12206-021-0410-x

Received December 1st, 2020
Revised February 18th, 2021
Accepted February 21st, 2021

† Recommended by Editor No-cheol Park

A study on squeal noise reduction considering the pad shape of the disc brake system for urban railway vehicles

Seoyeon Ahn[1], Chanhyuk Nam[1], Sungjin Choi[1], Daekwon An[2], Ingi Kim[3], Kyungsoo Seo[4] and Changhyun Sohn[5]

[1]Korea Automotive Technology Institute, Cheonan, Korea, [2]Sangsin Brake Co., Ltd, Daegu, Korea, [3]KORAIL, Daejeon, Korea, [4]Seoul Metro, Seoul, Korea, [5]Kyungpook National University, Daegu, Korea

Abstract In this paper, to help reduce the squeal noise produced during the braking of urban railway vehicles, the shape of the disc brake pad was investigated to relieve contact stress. To analyze the disc brake system to identify the source of the squeal noise, a finite element model of the disc brake system was used, including the peripheral brake parts to increase accuracy. A complex eigenvalue analysis was performed to predict squeal noise generation. Verification was carried out using domestic urban railway field test results to confirm the accuracy of the analysis model. A pad shape that relieves contact stress is proposed to reduce squeal noise produced by nonuniform contact between the disc and pad. The results of this study can be utilized for future studies on squeal noise reduction.

1. Introduction

When urban railway vehicles brake, noises of 1000 Hz and higher are produced by friction between the brake disc and pad. This is known as squeal noise [1, 2]. This squeal noise is one of the most sensitive noises, typically in the audible frequency range of 20 Hz-20000 Hz [3]. Squeal noise produced by urban railway vehicles is a major source of public noise, and causes discomfort to passengers and residents near stations, and as a result has attracted increasing attention as an environmental and social issue of increasing importance [4, 5]. In addition, railway environment noise standards are gradually becoming increasingly strict, to improve the quality of life of residents near railways and to strengthen their rights [6]. Although various studies on the brake squeal noise of urban railway vehicles have been carried out recently, no clear cause analyses or detailed technical solutions have been presented yet [7-10].

A representative prediction method that can be used for studying brake squeal noise is the widely used complex eigenvalue analysis method [11]. This method calculates a predicted result in the frequency domain, based on the premise that an unstable mode can be created by the merging of two neighboring natural modes into the same frequency. This occurs due to a self-excited oscillator resulting from friction in the system parameters. The eigenvalue analysis method has been widely employed, including Chen et al. [12], Hoffman et al. [13], Kang [14], and Ghazaly et al. [15]. However, studies of urban railway vehicles comparing experimental and simulation results are presently lacking, due to constraints of cost, time, and safety.

This study conducted an FEM based complex eigenvalue analysis to predict the squeal noise of the disc brake system of an urban railway vehicle, and a correlation was conducted with field test results for verification. The analysis model included the peripheral parts of the lining head, lever, fixed support, and hanger in order to improve the accuracy of the disc-pad model. Based on these results, the pad shape was improved to reduce squeal noise by relieving stress caused by disc-pad contact.

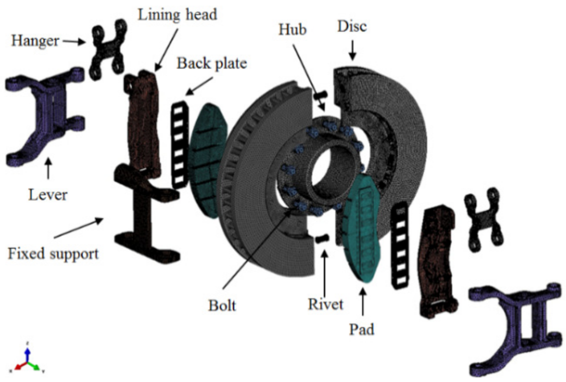

Fig. 1. Disc brake system components.

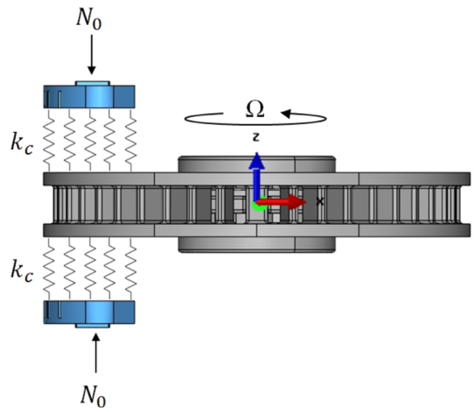

Fig. 2. Schematic of disc brake system.

2. Complex eigenvalue analysis and field test

2.1 Squeal noise analysis for the disc brake system

2.1.1 Schematic of the disc brake system

The disc brake system of an urban railway vehicle is composed of a disc, pad, and peripheral parts that can apply braking pressure, as shown in Fig. 1. Typically, squeal noise analyses of the disc brake system have used disc and pad models [16-18].

In the disc brake system of urban railway vehicles, the pad is fixed except in the z-axis direction, as shown in Fig. 2. The pad makes contact with the disc by applying a normal force N_0, and contact stiffness K_c exists between the pad and disc. When the disc rotates at a speed of Ω, friction is produced between the fixed pad and the rotating disc, and the coefficient of kinematic friction μ_k produced here is independent of N_0.

Thus, the friction force F on the system can be expressed as Eq. (1) where V_s is the sliding speed between the disc and pad [19, 20].

$$F = -\mu_k N_o \frac{V_s}{V_s} . \tag{1}$$

In this paper, a complex eigenvalue analysis was conducted using FEM, considering the contact and friction of the disc brake system of urban railway vehicles, in order to predict squeal noise. The general purpose analysis software ABAQUS was used for the complex eigenvalue analysis [21, 22], which was composed of four steps in total. The first step was a contact analysis between the disc and pad resulting from brake cylinder pressure, the second step was a friction analysis of the disc and pad considering the disc rotation, the third step was a natural frequency and modal analysis ignoring the damping and friction effects of the disc and pad, and the fourth step was a continuous complex eigenvalue analysis considering the friction between the disc and pad [23].

The equation of motion of the brake system for squeal noise analysis is as shown in Eq. (2) [24].

$$[M]\ddot{\vec{u}} + [C]\dot{\vec{u}} + [K]\vec{u} = [F] . \tag{2}$$

Here, $[M]$ is the mass matrix, $[C]$ is the damping matrix, $[K]$ is the stiffness matrix, u is the general displacement vector, and $[F]$ is the force matrix.

Friction between the disc and pad can be expressed as Eq. (3), where $[K_f]$ is the stiffness matrix with friction considered.

$$[F] = [K_f]\vec{u} . \tag{3}$$

Substituting Eq. (3) into Eq. (2) results in Eq. (4). Here, $[K]$ becomes an asymmetric matrix due to the friction and the eigenvalue of the system can be a complex number.

$$[M]\ddot{\vec{u}} + [C]\dot{\vec{u}} + [K - K_f]\vec{u} = [F] . \tag{4}$$

The complex eigenvalue analysis system considering Eq. (4) can be expressed as Eq. (5).

$$\left(\lambda^2[M] + \lambda[C] + [K]\vec{y}\right) = 0 . \tag{5}$$

Here, λ is the eigenvalue, $\vec{y}$ is the eigenvector, and λ takes the form of complex numbers with real and imaginary numbers, as shown in Eq. (6). $\mathrm{Im}(\lambda)$ refers to the natural frequency of the system and $\mathrm{Re}(\lambda)$ becomes the criterion for determining system stability and instability.

$$\lambda = \mathrm{Re}(\lambda) + i\,\mathrm{Im}(\lambda) . \tag{6}$$

Also, $\vec{u}$ can be expressed as Eq. (7), where a positive value $\mathrm{Re}(\lambda)$ indicates system instability, and the potential for squeal noise generation. N_a is the total number of modes used.

$$\vec{u} = \sum_{n=1}^{N_a} \overrightarrow{y_n} e^{\mathrm{Re}(\lambda_n t)} e^{i(\mathrm{Im}(\lambda_n t))} . \tag{7}$$

Table 1. Natural frequency analysis results of pad.

Pad	1st mode	2nd mode	3rd mode	Pad test
Test [Hz]	1118	1982	4204	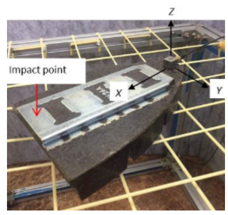
Simulation [Hz]	1141	2061	4323	
Error [%]	2.0	4.0	2.8	
Mode shape	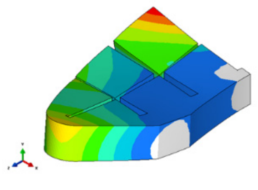	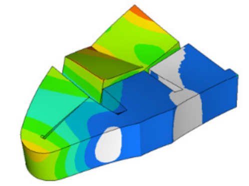	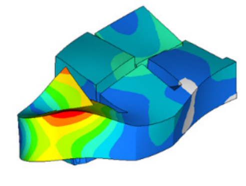	

Table 2. Natural frequency analysis results of disc.

Disc	1st mode	2nd mode	3rd mode	Disc test
Test [Hz]	484	1006	1550	
Simulation [Hz]	464	1027	1599	
Error [%]	4.1	2.1	3.2	
Mode shape	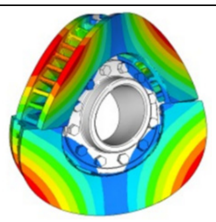	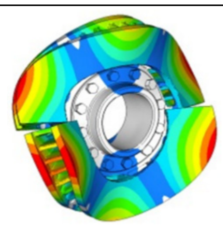	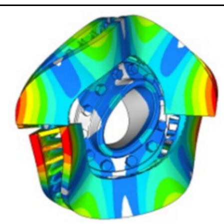	

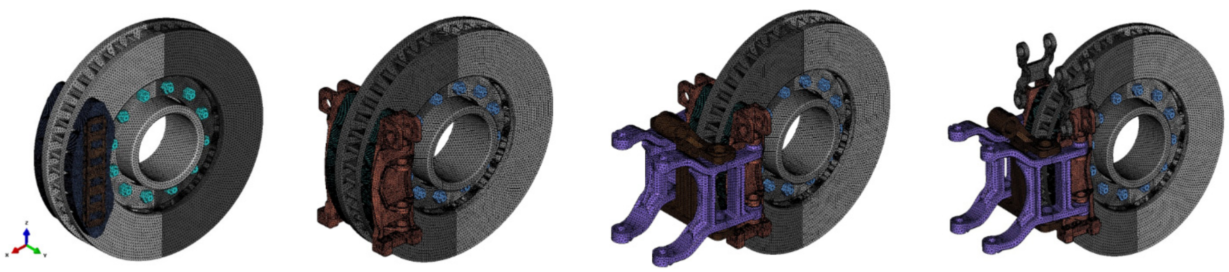

(a) Base (b) Case 1 (c) Case 2 (d) Case 3

Fig. 3. Finite element method model of disc brake system.

2.1.2 Analysis model composition

In this study, ABAQUS was used for the FEA modeling using tetra elements. To ensure the accuracy of squeal noise generation, cases 1-3 were prepared using a base model, as shown in Fig. 3, where the peripheral parts of the lining head, hanger, lever, and fixed support of the brake system were selectively applied and then compared with the field test results.

The base model was composed of two semicircle shaped cast-iron discs fastened with rivets, hubs, and bolts, with the pad and back plate attached. The model was composed of 730371 elements and 175934 nodes. Case 1 added the lining head to the base model, case 2 added the fixed support and lever to case 1, and case 3 added the hanger to case 2.

Modal testing and natural frequency analyses under the free-free condition were conducted for the disc brake components and the results are shown in Tables 1-3. The errors for each mode for both the analysis and experiment results were below 5.0 %. The density and Young's modulus values used for each part in the analysis are listed in Table 4.

2.1.3 Complex eigenvalue analysis

For the complex eigenvalue analysis, the conditions of squeal noise generation were considered. A disc rotation speed of 5rad/sec and the pressure of 5.0 bar from the brake cylinder were applied to the vertical direction of the contact surface, and the friction coefficient of 0.35 was applied between the disc and pad [20]. A hinge element was applied to the fastenings between the lining head and lever, lining head and hanger, and fixed support and lever, and they were constrained so that only axial rotation was possible.

The contact stiffness, which refers to deformation per contact pressure when applying the brake pressure, was calculated

Table 3. Natural frequency analysis results of lining head.

Lining head	1st mode	2nd mode	3rd mode	Lining head test
Test [Hz]	406	568	1027	
Simulation [Hz]	398	596	1070	
Error [%]	1.9	5.0	4.1	
Mode shape			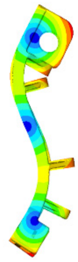	

Table 4. Material properties of disc brake components.

	Density [kg/m^3]	Young's modulus [MPa]	Poison's ratio
Pad	2516	5200	0.25
Disc	7550	120000	0.30
Lining head	9379	200000	0.30
et al. (steel)	7850	200000	0.30

Table 5. Data acquisition system.

Equipment	Model	Specification
Microphone	B&K 2671	1EA
Accelerometer	PCB353B15	1EA
Data acquisition system	LMS SCADAS	3CH
GPS	-	1EA

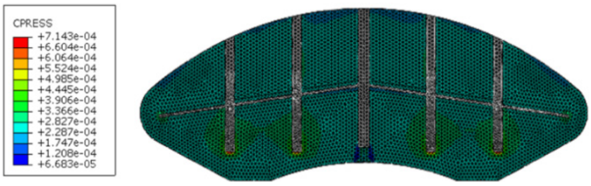

Fig. 4. Contact pressure.

using Eq. (8) [25].

$$K_c = P_{c\max} / u_{\max} . \quad (8)$$

Here, $P_{c\max}$ is the maximum contact pressure and $u_{\max}$ is the maximum deformation. The contact pressure was obtained as shown in Fig. 7, when pressure is applied to the pad so that it is in close contact with the disc. The contact stiffness of 3.57e+11N/m^3 was applied.

2.2 Validation field test

2.2.1 Squeal noise measurement subject

Measurement of the squeal noise during braking was carried out on an EOD (electric operating device) applied to a train in operation on an actual domestic urban railway line. The squeal noise was measured when the air brake was applied during braking immediately before stopping at each station.

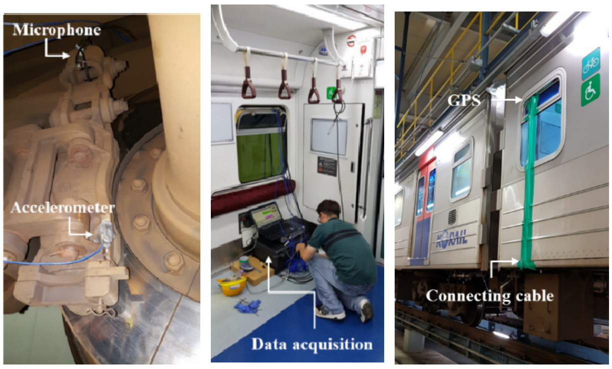

(a) Microphone & accelerometre (b) LMS DAQ (c) GPS

Fig. 5. Data measurement equipment setup.

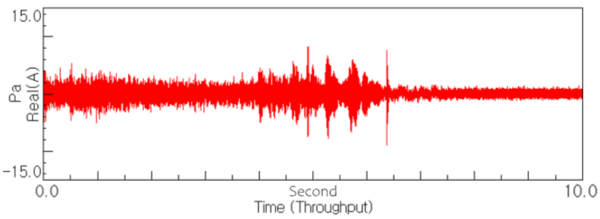

(a) Time - sound pressure

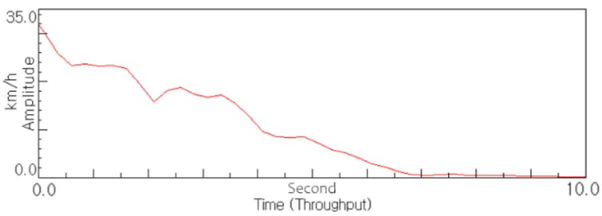

(b) Time - speed

Fig. 6. Sound pressure and speed.

 DOI 10.1007/s12206-021-0410-x

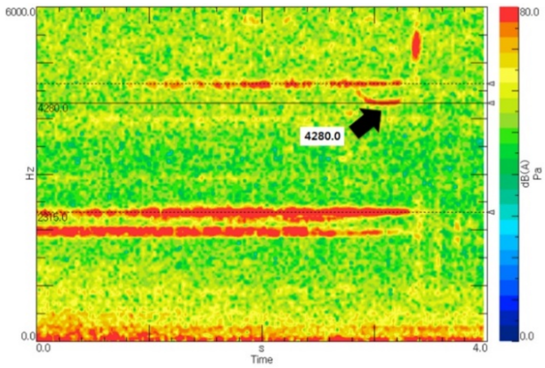

(a) Sound pressure

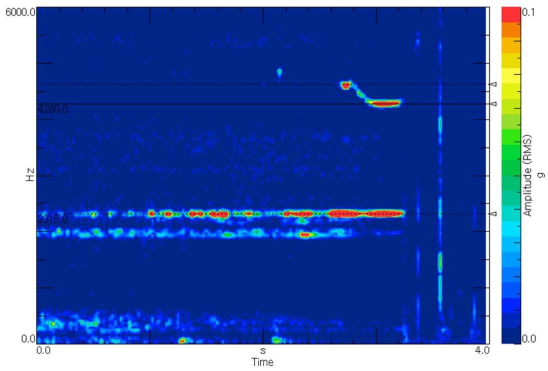

(b) Accelerometer

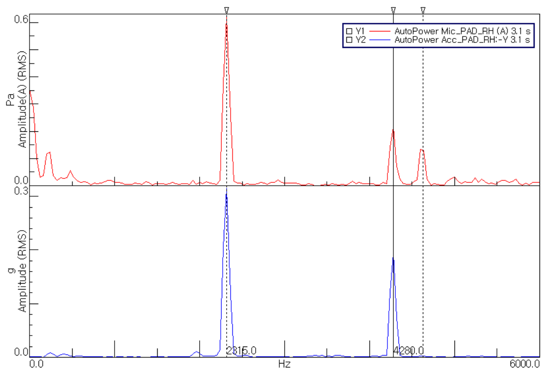

(c) FFT analysis

Fig. 7. Brake field test data of A station.

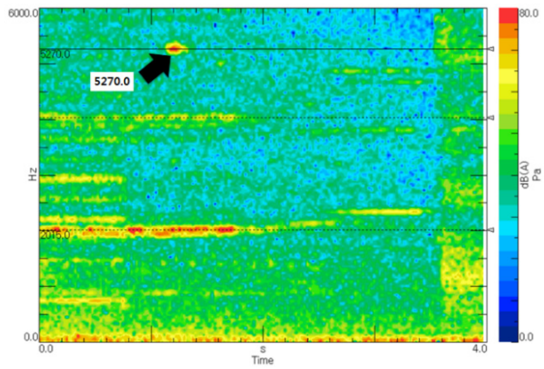

(a) Sound pressure

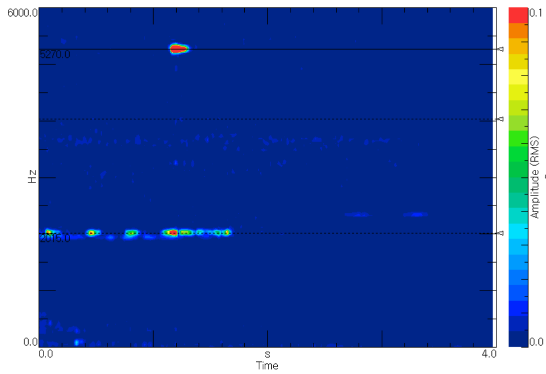

(b) Accelerometer

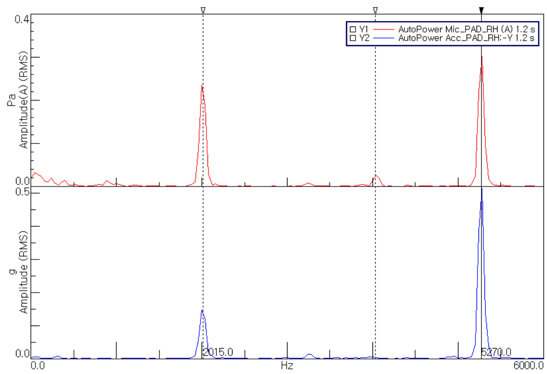

(c) FFT analysis

Fig. 8. Brake field test data of B station.

The components of the measurement system used in this study are listed in Table 5. As shown in Fig. 5(a), noise measurement sensors including a microphone and accelerometer were installed on the lining head of bogie 2. Fig. 5(b) shows the installation of the DAQ (data acquisition) within the subject vehicle car [26]. Also, GPS was installed to collect the speed data of the urban railway vehicle.

2.2.2 Noise measurement results

For the squeal noise measurement, noise and speed data were acquired for approximately 10 seconds from the entry of the urban railway vehicle into each station building, until the point of complete stop, as shown in Fig. 6. The sound pressure was expressed in Pa units, and A-weighting used for noise level measurements was applied for the weighting network. From the analysis of the sound pressure and speed data, it was found that high sound pressure is produced just before braking.

Figs. 7 and 8 show the measured noise and vibration data for stations A and B, respectively, on the domestic urban railway line. Here, (a) is the sound pressure data measured using the microphone, (b) is the vibration data measured using the accelerometer, and (c) is the FFT (fast Fourier transform) graph of the sound pressure and acceleration at the time point of squeal noise generation.

In color maps (a) and (b), the noise and vibration distributions revealed that strong squeal noises higher than 80 dB(A) and vibrations of 4280 Hz and 5270 Hz were produced before the urban railway vehicle stopped. To determine the source of the squeal noise, figures (c) showed that the sound pressure and vibration were simultaneously obtained from both the microphone and accelerator sensor data. The noise and vibration at 2315 Hz were identified to be due to friction with the rail.

2.3 Analysis and experiment result analysis

The predicted results of the complex eigenvalue analysis conducted for the instability analysis of the disc brake system are shown in Fig. 9. The x-axis in the graph is the unstable frequency, and the y-axis is the positive real part of the unstable frequency. The analysis model of the brake squeal noise investigated the results from cases 1-3, where peripheral parts were added to the base model, which was the disc-pad model, as shown in Fig. 2.

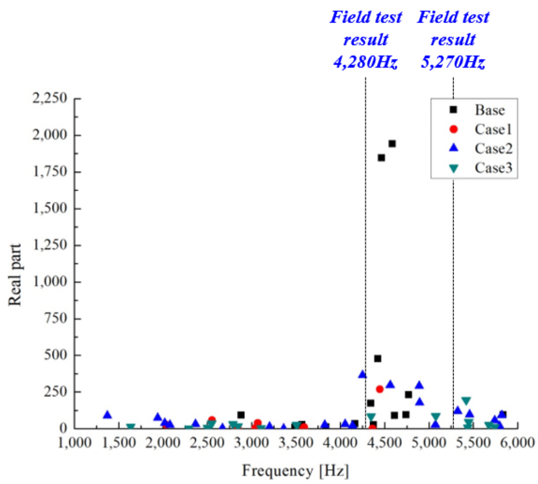

Fig. 9. Unstable frequency results of model.

The maximum positive real parts for the base model, cases 1-3 were predicted to be 1942 at 4589 Hz, 269 at 4446 Hz, 366 at 4251 Hz, and 195 at 5418 Hz, respectively.

The brake squeal noise analysis model was verified for 4280 Hz and 5270 Hz, when squeal noise was generated in the field test. The analysis results showed that the error with the field test was within 10 %. In the analysis results, the noise frequency was calculated based on the maximum real number.

The maximum positive real number for the base model was 1942 at 4589 Hz, which had an error of 7 % with the field test result of 4280 Hz, and 231 at 4773 Hz, which had an error of 9 % with the field test result of 5270 Hz. For case 1, the positive real number 269 was predicted at 4446 Hz, which had an error of 4 % with the field test result of 4280 Hz. A positive real number did not occur near the test result of 5270 Hz.

For case 2, the positive real number 366 was predicted at 4251 Hz, which had an error of 1 % with the field test result of 4280 Hz, and the positive real number 291 was predicted at 4892 Hz, which had an error of 7 % with the field test result of 5270 Hz. For case 3, the positive real number 84 was predicted at 4346 Hz, which had an error of 1 % with the field test result of 4280 Hz, and the positive real number 195 was pre-

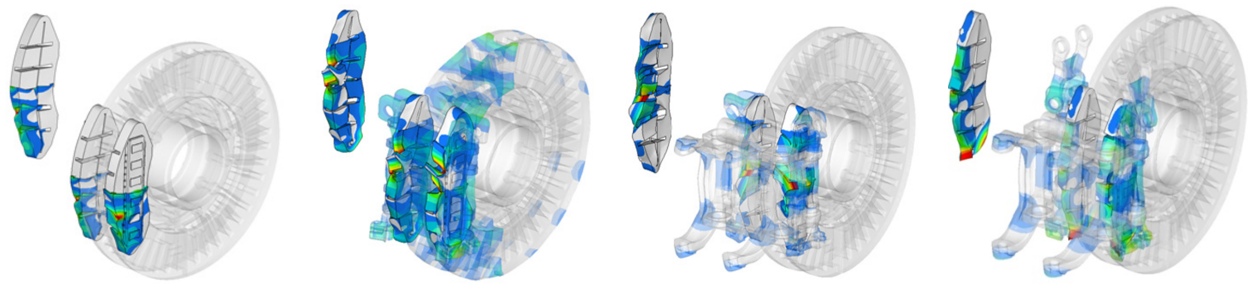

(a) Base (b) Case 1 (c) Case 2 (d) Case 3

Fig. 10. Mode shape of 4280 Hz.

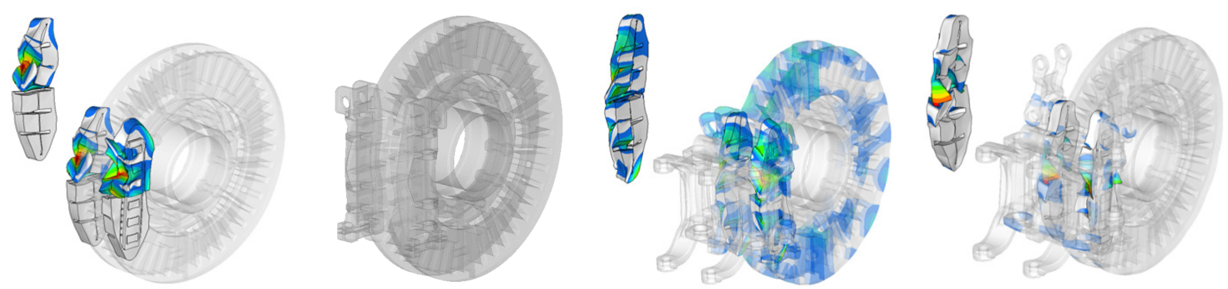

(a) Base (b) Case 1 (c) Case 2 (d) Case 3

Fig. 11. Mode shape of 5270 Hz.

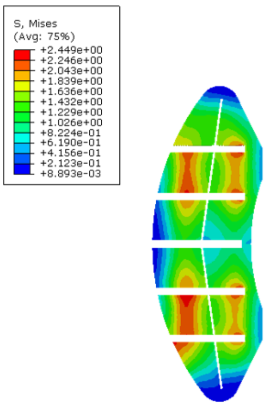

(a) Contact analysis

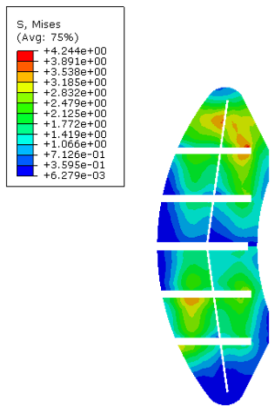

(b) Rotation analysis

Fig. 12. Stress distribution on pad.

dicted at 5418 Hz, which had an error of 2 % with the field test result of 5270 Hz. Figs. 10 and 11 show the mode shapes for each frequency.

2.4 Squeal reduction analysis

2.4.1 Proposed pad shapes

This study investigated methods for reducing squeal noise by reducing system instability through changes in the pad shape based on case 3, which had the smallest error with the field test results. To derive the best pad shapes for squeal noise reduction, contact and friction analyses of the disc and pad were carried out to determine the stress distribution on the contact surface of the pad. Fig. 12 shows the stress distribution on the contact surface of the pad, and it was found that the stress was concentrated near the slots.

Local stress concentrations create deformation of the pad shape, inducing nonuniformity in the contact surface, which in turn negatively impacts squeal noise. To evenly distribute the concentrated stress, chamfers of various forms were applied near the slots, as shown in Fig. 13. 45° chamfers were applied to the slots in case A. For case B, 60° chamfers were additionally applied to those in case A. For case C, 36° chambers were applied to each end of the pad where it comes into contact with the disc.

2.4.2 Analysis results

To analyze the squeal noise in relation to the pad shape, the stress distribution on the contact surface of the pad was obtained from the contact analysis between the disc and pad, and a rotation analysis considering the disc rotation.

The results of the analysis of contact between the disc and pad are shown in Fig. 14. It predicted that the stress would be more evenly distributed for cases A and especially B than that of the base pad. Also, case C showed a similar stress distribution to that of the baseline pad.

The analysis results considering the disc rotation are shown in Fig. 15. The pad surface deformed in the rotation direction

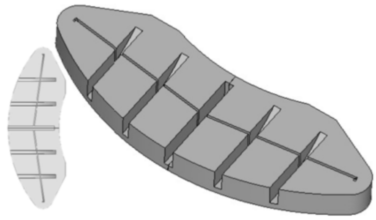

(a) Base

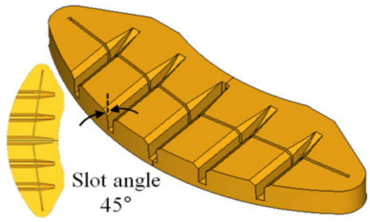

(b) Case A

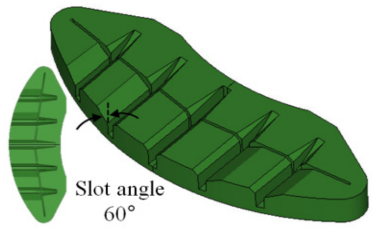

(c) Case B

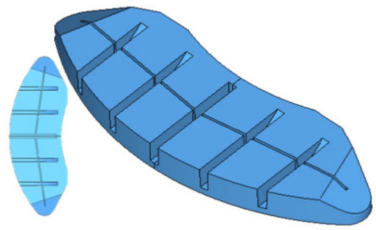

(d) Case

Fig. 13. Modified pad shape.

and stress concentrations occurred locally near the slots. In cases A and B, stress concentrations occurred near the chamfers. In case C, although it was observed that stress concentrations occurred in the upper area of the pad where the contact angle with the disc for each end of the pad were varied, other areas were predicted to have uniform stress distributions.

The complex eigenvalue analysis results for the pad shape are shown in Fig. 16, and were found to have errors within 10 % when compared with the field test results. Compared to case 3 with the base pad shape, case A showed an increase of 4 % to 88 at 4286 Hz and a 33 % decrease to 130 at 5394 Hz with regard to positive real numbers. For case B, at 4354 Hz, the positive real number decreased by 51 % to 41, and at 5730 Hz, it decreased by 33 % to 69 when compared to the base pad shape. For case C, there was no positive real part in the 4289 Hz band, and the positive real number decreased by 7.5 % at 5530 Hz to 180 in comparison to the base pad shape. Figs. 17 and 18 show the corresponding pad mode shapes.

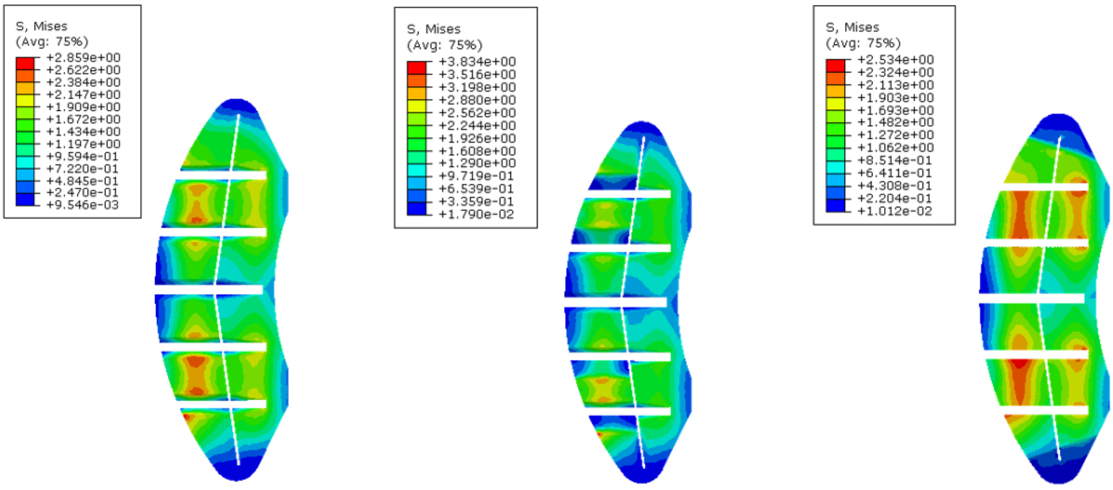

(a) Case A (b) Case B (c) Case C

Fig. 14. Stress distributions of contact analysis.

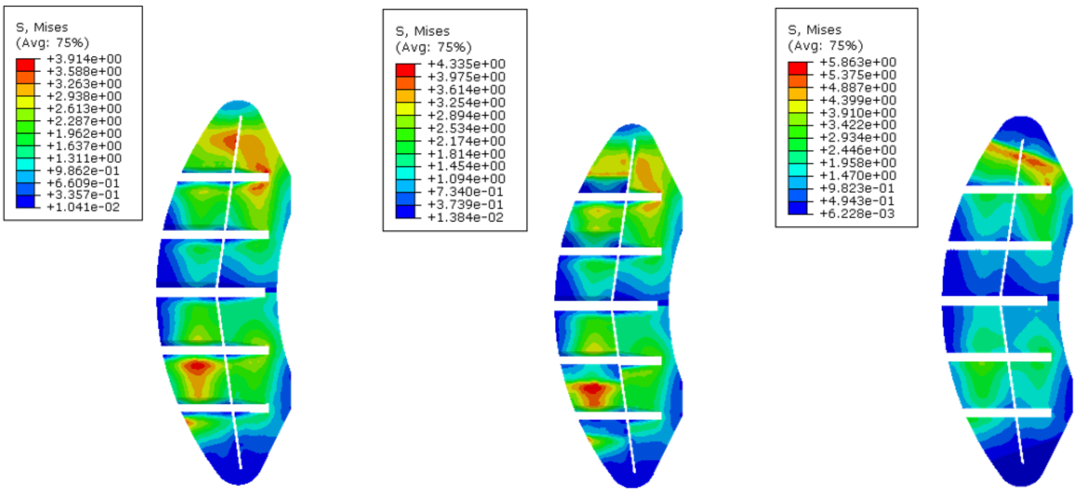

(a) Case A (b) Case B (c) Case C

Fig. 15. Stress distributions of rotation analysis.

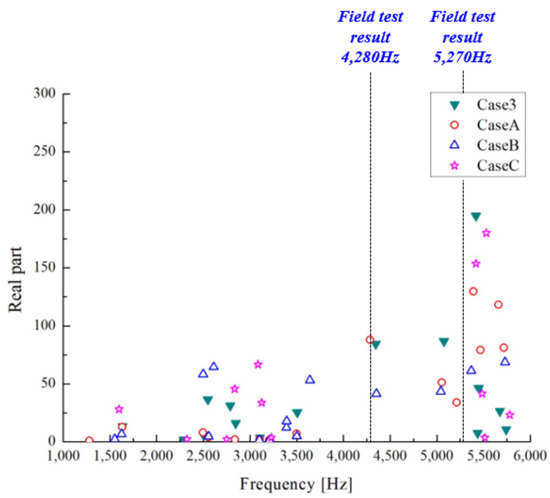

Fig. 16. Unstable frequency results of modified pad shape.

3. Conclusions

In this paper, an FEM based complex eigenvalue analysis was carried out to predict the squeal noise produced by the disc brake system of an urban railway vehicle during braking. The analysis results were then compared with field test results. In addition to the disc-pad, peripheral parts including the lining head, lever, fixed support, and hanger were additionally included in the model to avoid the inaccuracies that occur when only the basic disc-pad system is considered, as in previous studies. This resulted in improved accuracy in comparison with the field test results.

Pad shapes were proposed to reduce squeal noise by relieving the contact stress between the pad and disc. Analysis of the proposed shapes predicted reductions in squeal noise. The following conclusions were obtained in this study.

1) With regard to the squeal noise measured right before

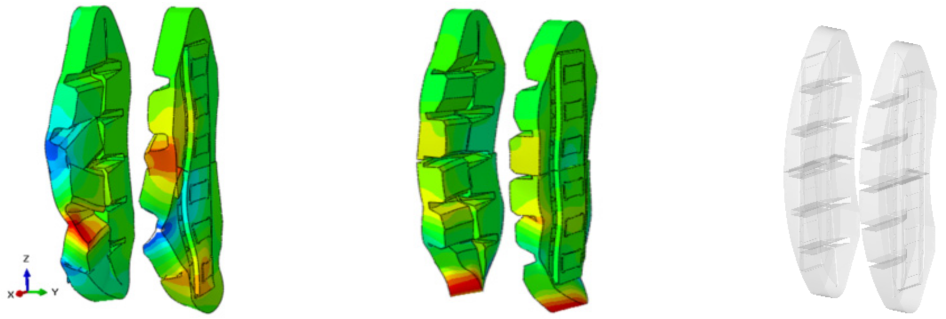

(a) Case A (b) Case B (c) Case C

Fig. 17. Mode shape of 4280 Hz.

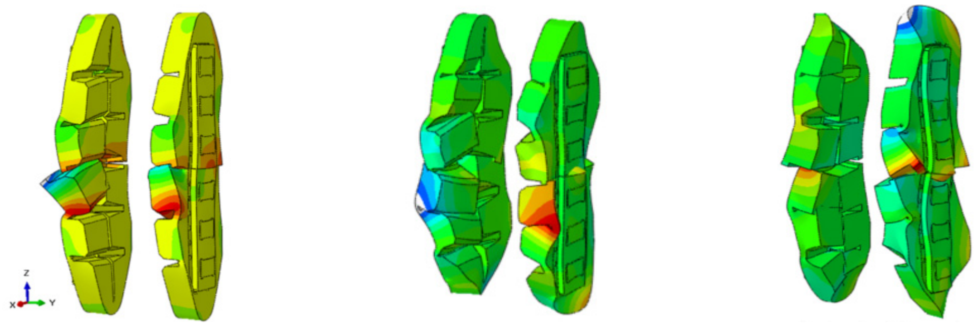

(a) Case A (b) Case B (c) Case C

Fig. 18. Mode shape of 5270 Hz.

braking during the field test, sound pressure and frequency analyses revealed that squeal noise of higher than 80 dB(A) and vibrations occurred at 4280 Hz and 5270 Hz.

2) The analysis models cases 1-3 for the squeal noise generation prediction was composed by taking into consideration the disc-pad and other peripheral parts such as the lining head, lever, fixed support, and hanger.

3) For case 3 that contained all peripheral parts of the lining head, lever, fixed support, and hanger, which was predicted to occur squeal noise at 4346 Hz and 5418 Hz, has errors of 2 % and 3 %, respectively, with the field test results. Through this, it was determined that the accuracy of the squeal noise prediction increased when the peripheral parts of the brake system were taken into consideration.

4) Case A-C were composed to reduce squeal noise by considering the shape of the pad that relieves concentrated stress. For case B where chamfer is applied to the slot of the case 3 brake pad, it was predicted that squeal noise would occur at 4354 Hz and 5730 Hz, and positive real number were reduced by 51 % in the 4280 Hz band and 65 % in the 5270 Hz band than in case 3. Therefore, it was predicted that squeal noise occurrence can be reduced by evenly distributing the concentrations of contact stress, which is relatively caused by instability, through the application of chamfers on the slots.

Acknowledgments

This work was financially supported by the Railroad Technology Research program (20RTRP-B123170-06) under the Korea Agency for Infrastructure Technology Advancement, Republic of Korea.

References

[1] M. Triches Jr., S. N. Y. Gerges and R. Jordan, Reduction of squeal noise from disc brake systems using constrained layer damping, *Brazilian Society of Mechanical Sciences and Engineering*, 26 (3) (2004) 340-348.

[2] L. B. Shi, F. Wang, L. Ma, Q. Y. Liu, J. Guo and W. J. Wang, Study of the friction and vibration characteristics of the braking disc/pad interface under dry and wet conditions, *Tribology International*, 127 (2018) 533-544.

[3] F. Bergman, M. Eriksson and S. Jacobson, Influence of disc topography on generation of brake squeal, *Wear*, 225 (1999) 621-628.

[4] J. M. Feild and J. G. Sinou, The response to railway noise in residential areas in Great Britain, *J. Sound Vib.*, 85 (2) (1982) 177-255.

[5] E. Denimal, J.-J. Sinou, S. Nacivet and L. Nechak, Squeal analysis based on the effect and determination of the most influential contacts between the different components of an automotive brake system, *International Journal of Mechanical Sciences*, 151 (2019) 192-312.

[6] *http://www.me.go.kr* (Accessed 30 June 2015).

[7] R. A. Ibrahim, Friction-induced vibration, chatter, squeal, and chaos. Part 2. Dynamics and modeling, *Appl. Mech.*, 47 (7)

(1994) 227-253.
[8] O. Chiello et al., Squeal noise generated by railway disc brakes: experiments and stability computations on large industrial models, *Proceedings of Meetings on Acoustics ICA2013*, 19 (1) (2013) 065049.
[9] X. Liu and P. A. Meehan, Investigation of squeal noise under positive friction characteristics condition provided by friction modifiers, *J. Sound Vib.*, 37 (2016) 393-405.
[10] H. Guo, Y. S. Wang, N. N. Liu, R. P. Yu, H. Chen and X. T. Liu, Active interior noise control for rail vehicle using a variable step-size median-LMS algorithm, *Mechanical Systems and Signal Processing*, 109 (2018) 15-26.
[11] J. Nam and J. Kang, Semi-analytical approach for brake squeal of a rail pad, *Journal of Mechanical Science and Technology*, 34 (8) (2020) 3147-3153.
[12] F. Chen, J. Chern and S. Swaze, Modal coupling and its effect on brake squeal, *SAE Technical Paper No. 2002-01-0922* (2002).
[13] N. Hoffmann, M. Fischer, R. Allgaier and L. Gaul, A minimal model for studying properties of the mode-coupling type instability in friction induced oscillations, *Mechanics Research Communications,* 29 (2002) 197-205.
[14] J. Kang, Squeal analysis of gyroscopic disc brake system based on finite element method, *Mechanical Science*, 51 (4) (2009) 284-294.
[15] N. M. Ghazaly, S. Mohammaed and A. M. Afd-El-Tawwab, Understanding mode-coupling mechanism of brake squeal using finite element analysis, *Engineering Research and Application*, 2 (1) (2012) 241-250.
[16] S. Oberst, J. C. S. Lai and S. Marburg Guidelines for numerical vibration and acoustic analysis of disc brake squeal using simple models of brake systems, *J. Sound Vib.*, 332 (2013) 2284-2299.
[17] H. Lü and D. Yu, Brake squeal reduction of vehicle disc brake system with interval parameters by uncertain optimization, *J. Sound Vib.*, 333 (2014) 7313-7325.
[18] L. Nechak, F. Gillot, S. Besset and J.-J. Sinou, Sensitivity analysis and kriging based models for robust stabilityanalysis of brake system, *Mechanics Research Communications*, 69 (2015) 136-145.
[19] N. M. Kinkaid, O. M. O'Reilly and P. Papadopoulos, Automotive disc brake squeal, *J. Sound Vib.*, 267 (2003) 105-166.
[20] J. Y. Kang, Moving mode shape function approach for spinning disk and asymmetric disc brake squeal, *Sound and Vibration,* 424 (2018) 48-63.
[21] A. AbuBakar and H. Ouyang, Wear prediction of friction material and brake squeal using the finite element method, *Wear*, 264 (11-12) (2008) 1069-1076.
[22] Dassault Systèmes*, ABAQUS Version 2019*, Documentation (2019).
[23] S. W. Kung, K. B. Dunlap and R. S. Ballinger, Complex eigenvalue analysis for reducing low frequency brake squeal, *SAE Technicl Paper Series,* No. 2000-01-0444 (2000).
[24] S. Y. Ahn et al., Study on parameter optimization of brake pad for squeal noise reduction for urban rail vehicle brake system, *Journal of the Korean Society Railway*, 22 (1) (2019) 1-10.
[25] V. Lugt and D. Neil, Analytical and experimental study of automotive disc brake squeal vibration, *Master Thesis*, Purdue University (2004).
[26] Siemens*, LMS SCADAS Version 14A, User Guide* (2014).

Seoyeon Ahn completed the Ph.D. degree in Mechanical Engineering from Kyungpook National University. She is a researcher of the Korea Automotive Technology Institute and is responsible for the CAE analysis and technical development of chassis design.

Chanhyuk Nam completed the Ph.D. degree in Mechanical Engineering from Korea University. He is a Principal Researcher of vehicle-platform R&D center in Korea Automotive Technology Institute. His research interest is the vehicle dynamics and chassis design.

Sungjin Choi graduated the Ph.D. degree in Mechanical Engineering from Ajou University. He is a Vice President of Convergence Technology R&D Center in Korea Automotive Technology Institute. His research interest is the vehicle dynamics and chassis design.

Daekwon An received the M.S. degree in the Department of Engineering Technology, Mechanical Engineering Major Graduate School of Industry, Kyungpook National University. He is currently a Gen. Manager of R&D and OE Sales Team in SANGSIN BRAKE. His research interest is vehicle-component design and development.

In-ki Kim received his bachelor's degree in electrical and electronic engineering at Kwangwoon University. He is currently one of the members of the Technical Research Department of the Korea Railroad Corporation (KORAIL) researchers and his research interests are field simulation and experimentation on reducing friction noise and disc aggression.

Kyoungsoo Seo is a Senior Researcher at the Railway Research Institute of Seoul Metro, Seoul, Korea. He received his Ph.D. in Business Administration from Hanyang University. His research interests include operations management, efficiency, and productivity on metro operations, maintenance, and management.

Chang Hyun Sohn received his M.Sc. and Ph.D. in Mechanical Engineering from KAIST in 1985, and 1991, respectively. He worked in ADD for 3 years. He also worked in University of Cambridge as a visiting Assistant Professor in 1996. He is currently a Professor at the Department of Mechanical Engineering at Kyungpook National University, Daegu, South Korea. His research interests include computational fluid dynamics, particle image velocimetry, flow induced vibration, Lattice Boltzmann method, parallel computation, and thermal hydraulics.